JOURNAL OF CATALYSIS 140, 121–135 (1993)

An Auger Electron Spectroscopy Study of the Activation of Iron Fischer–Tropsch Catalysts

I. Hydrogen Activation[1]

ALLEN G. SAULT

Fuel Science Department 6211, Sandia National Laboratories, Albuquerque, New Mexico 87185

Received July 23, 1992; revised October 29, 1992

Activation procedures can have a dramatic effect on the activity of iron-based catalysts for Fischer–Tropsch (F–T) synthesis. CO conversion over a 100 Fe/3 Cu/0.2 K catalyst (parts by weight) can vary by nearly a factor of 3, depending on activation. In contrast, a 100 Fe/5 Cu/4.2 K/25 SiO_2 catalyst displays only minor variations in activity with activation conditions. An ultra-high vacuum surface analysis chamber coupled to an atmospheric pressure reactor has been used to measure the surface compositions of these catalysts following various hydrogen activation procedures. Activation of the 100 Fe/3 Cu/0.2 K catalyst in H_2 results in rapid reduction of iron to the metallic state, and segregation of sulfur to the catalyst surface. The sulfur arises from bulk sulfate impurities present in the metal nitrates used to prepare the catalyst. Sulfur coverage increases with both activation time and temperature, due to an increase in the rate of sulfur diffusion with temperature. F–T activity of this catalyst varies inversely with sulfur coverage, consistent with the well-known poisoning effect of sulfur on F–T synthesis. For the 100 Fe/5 Cu/4.2 K/25 SiO_2 catalyst no significant variations in surface composition are observed as a function of hydrogen activation temperature, consistent with the absence of any variations in catalyst activity. Only partial reduction of iron to a mixture of FeO and Fe_3O_4 is observed for this catalyst for all activation conditions investigated. Using electron beam effects to remove potassium and silica shows that one or both of these components inhibits reduction of iron to the metallic state in the 100 Fe/5 Cu/4.2 K/25 SiO_2 catalyst. The difference in sensitivity of the two catalysts to activation conditions is explained by differences in surface area and reducibility of the two catalysts. Reduction of the 100 Fe/3 Cu/0.2 K catalyst is accompanied by a severe loss of surface area, such that sulfur segregation can result in substantial sulfur coverages on the surface. The 100 Fe/5 Cu/4.2 K/25 SiO_2 catalyst maintains high surface area during activation, and not enough sulfur is available to form significant coverages on the surface.

1. INTRODUCTION

Promoted iron catalysts are commonly used for Fischer–Tropsch (F–T) synthesis. Copper, potassium, and silica are frequently employed as promoter species, either singly or in combination. Copper is added to aid in the reduction of iron (*1–4*), potassium promotes CO dissociation and carbon chain growth (*1–3*, *5–8*), and silica is a structural promoter added to stabilize catalyst surface area (*1*, *3*, *8*). Even though the number of different iron catalyst formulations which have been investigated for F–T synthesis is enormous, there does not yet appear to be a general consensus as to the optimum catalyst composition, or even the desired product distribution. In addition, questions regarding the effects of variations in catalyst activation and reaction conditions are still open. Because of the large number of parameters involved in the development of F–T catalysts, a great deal of work remains to be done before the factors affecting catalyst performance are fully understood.

[1] This work was performed at Sandia National Laboratories for the U.S. Department of Energy under Contract DE-AC04-76DP000789.

0021-9517/93 $5.00

In this paper and the following one (*9*), an investigation of one of these factors, namely, the effects of variations in activation procedure on the surface composition of iron based F–T catalysts, is reported. Two different catalysts were studied. F–T activity and selectivity for these catalysts, as measured by Bukur *et al.* (*10*, *11*), are summarized in Table 1. The first catalyst, a commercial catalyst manufactured by Ruhrchemie with a composition of 100 Fe/5 Cu/4.2 K/25 SiO_2 (parts by weight), shows little variation in activity and hydrocarbon selectivity with activation procedure (*10*). Activation in 1 atm of hydrogen at 220 or 280°C for 1 h, or in 1 atm of CO at 280°C for 12 h, all give initial CO conversions of 55–65% when tested in a fixed bed reactor at 250°C, 1.48 MPa total pressure, $H_2:CO$ = 2:3, and a space velocity of 2 Nl/g-catalyst · h. Tests in a slurry phase reactor with identical process conditions also show little sensitivity to activation conditions, although overall conversions are only 35–45% in the slurry phase. The second catalyst, with a composition of 100 Fe/3 Cu/0.2 K, displays wide variations in activity and selectivity with activation procedure (*11*). Initial CO conversion, measured in a fixed bed reactor at 250°C, 1.48 MPa total pressure, $H_2:CO$ = 1:1, and a space velocity of 2 Nl/g-catalyst · h, increases from 30% to 80% as activation conditions are varied. Surface compositions and surface areas of these two catalysts were measured after the activation treatments described above, using Auger electron spectroscopy (AES) and BET measurements, respectively. In this paper, the effects of hydrogen activation on the surface compositions of the two catalysts is reported. The following paper presents results for activation in CO (*9*). It will be shown that the variations in catalyst activity observed by Bukur *et al.* (*10*, *11*) correlate well with variations in surface composition, offering insights into the effects of catalyst activation on F–T activity.

TABLE 1

CO Conversion vs Activation for F–T Catalysts

Activation treatment	Initial CO conversion (%)	Hydrocarbon selectivities (wt%)			
		CH_4	C_2–C_4	C_5–C_{11}	$C_{12}+$
100 Fe/5 Cu/4.2 K/25 SiO_2[a]					
CO, 280°C, 12 h	55	5	22	19	54
H_2, 220°C, 1 h	59	6	21	29	44
H_2, 280°C, 1 h	64	9	24	47	20
100 Fe/3 Cu/0.2 K[b]					
CO, 280°C, 8 h	80	7	27	31	35
CO, 280°C, 24 h	80	7	26	23	44
H_2, 250°C, 8 h	66	14	40	39	7
H_2, 250°C, 24 h	60	12	39	42	7
H_2, 280°C, 8 h	44	14	45	37	4
H_2, 280°C, 24 h	30	11	39	40	10

[a] 250°C, 1.48 MPa, H_2:CO = 2:3, 2 Nl/g-catalyst · h, from Ref. (*10*).
[b] 250°C, 1.48 MPa, H_2:CO = 1:1, 2 Nl/g-catalyst · h, from Ref. (*11*).

There have been numerous studies of F–T synthesis on model iron catalysts using ultrahigh vacuum (UHV) analysis coupled with atmospheric pressure reactor studies. Particularly noteworthy are the works of Dwyer and co-workers (*4*, *5*, *12–14*) and Bonzel and co-workers (*6*, *7*, *15–18*), on both clean and potassium-promoted iron powders, foils, and single crystals. In addition, model studies have been reported which employ magnetite (Fe_3O_4) samples (*19*) and hematite (Fe_2O_3) powders (*20*). In contrast, the number of UHV studies of actual high-surface-area promoted F–T catalysts is relatively small (*21–24*). Most relevant to the present work are a thesis by Li (*21*) in which XPS was used to study the surface composition of a number of precipitated iron catalysts promoted by varying amounts of copper, potassium, and silica, and a study by Lox *et al.* (*22*), in which the surface composition of the commercial Ruhrchemie catalyst was investigated following activation and reaction. It has been shown that the 100 Fe/5 Cu/4.2 K/25 SiO_2 catalyst studied by Li displays activation behavior which is nearly identical to that of the Ruhrchemie catalyst (*25*).

2. METHODS

The experimental apparatus used in this study is shown schematically in Fig. 1. The

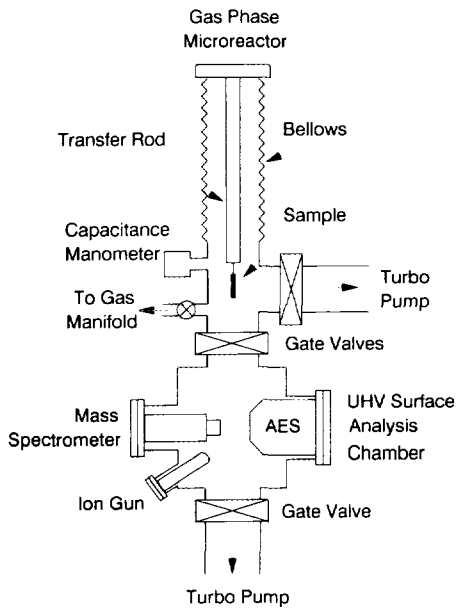

FIG. 1. Schematic diagram of the experimental apparatus.

system consists of an ultra-high vacuum (UHV) chamber (base pressure = 3×10^{-10} Torr, 1 Torr = 133.3 N/m^2) coupled to an atmospheric pressure gas-phase reactor. This arrangement allows catalyst samples to be subjected to realistic activation or reaction conditions, and then introduced into UHV for analysis without exposure to air. This capability is crucial to obtaining relevant information on the surface composition of working catalysts, as activated catalysts are often highly reactive toward oxygen.

The UHV chamber is equipped with a single-pass cylindrical mirror analyzer with an integral electron gun (Perkin–Elmer, Model C15-155) for Auger electron spectroscopy (AES), and an argon-ion gun (Hiden Analytical, Model IG20) and quadrupole mass spectrometer (Hiden Analytical, Model PC301) for secondary ion mass spectroscopy (SIMS) and residual gas analysis. Only AES was used in this study. Samples are mounted on the end of a long transfer rod coupled to a welded bellows assembly which allows movement between the reactor and the UHV analysis chamber. Sample temperature is measured with a chromel–alumel thermocouple spot welded to the sample.

Atmospheric pressure treatment of a sample is accomplished by first heating to the desired temperature in vacuum in order to remove any residual gases adsorbed on the sample. In this manner, buildup of these residual gases in the reactor during activation or reaction is minimized. Once the desired temperature is reached, the sample is isolated in the reactor (volume $\approx$500 cm^3) and the reactor is filled to the desired pressure with the reactant gases through the gas manifold. A capacitance manometer (0–1000 Torr) monitors reactor pressure. After completion of the activation or reaction, reactant gases are evacuated in stages using a mechanical pump and turbo pump. Sample temperature is held at the reaction temperature during evacuation to avoid readsorption of product gases. Once the reactor pressure falls below 5×10^{-6} Torr, the gate valve to the analysis chamber is opened and the sample lowered and cooled. Pressure in the analysis chamber is always allowed to fall to less than 5×10^{-8} Torr before any analysis is performed.

Two different F–T catalysts were studied in this work, with compositions of 100 Fe/3 Cu/0.2 K and 100 Fe/5 Cu/4.2 K/25 SiO_2, expressed as parts by weight of the various components. Catalyst compositions were verified by atomic absorption spectroscopy. Both of these catalysts are identical to the samples used in the reactivity studies of Bukur *et al.* (*10*, *11*). The catalysts are prepared by continuous precipitation of $Fe(NO_3)_3$ and $Cu(NO_3)_2$ with NH_4OH, followed by potassium loading by incipient wetness with a $KHCO_3$ solution, and silica loading by impregnation with a K_2SiO_3 solution (*11*, *21*). Samples were mounted by pressing approximately 30 mg of finely ground catalyst onto an etched tungsten mesh (Buckbee-Mears, 0.001 inch wires, 50 wires/inch) at 2000 psi, to form a porous disk approximately 0.5 cm in diameter. The

tungsten mesh was suspended between two electrical feedthroughs by means of copper clamps and heated by passing current through the mesh. A thermocouple was spotwelded to the mesh near the sample. Initial heating of the catalysts in vacuum always resulted in the evolution of water, necessitating outgassing prior to the activation studies. Outgassing was performed by slowly raising the sample temperature to 300°C, such that the chamber pressure always remained below 1×10^{-6} Torr. The sample was then held at 300°C until the chamber pressure fell below 5×10^{-8} Torr. Although water was the main species generated by outgassing, some evolution of NO, CO, and CO_2 was also observed. NO is presumably formed by decomposition of nitrate anions, since iron nitrate was used as a starting material in the catalyst preparation, while CO and CO_2 may be generated by reaction of adventitious carbon with oxygen contained in the as-prepared catalysts.

Prior to all activation treatments, the samples were heated to 300°C in 130 Torr O_2 for 3 h. This procedure simulated the calcining step employed by Bukur *et al.* (*10*, *11*), in their reactivity studies, and served to remove adventitious carbon and completely oxidize the iron in the samples to Fe_2O_3. Upon opening the gate valve following hydrogen activation treatments, the analysis chamber pressure typically rose to $>1 \times 10^{-7}$ Torr, mostly water and hydrogen. The catalyst samples, which were smooth, red-brown pellets upon pressing and after calcining, shrank and cracked significantly during activation and changed to a deep black color. Examination of the samples under an optical microscope after removal from the apparatus revealed shiny, metallic gray surfaces.

Activation treatments for times longer than four hours were done in several stages. This procedure allowed changes in surface composition to be monitored as a function of activation time, and also ensured that buildup of water in the reactor did not affect the results. The first stage of activation typically lasted four hours with subsequent activation stages lasting 6 h. It was found that a single sample could be used to study more than one activation condition. For both catalysts, recalcining at 300°C following activation restored the surface compositions to their original states, such that a second activation procedure could be studied. The order in which activation treatments were studied did not affect the results. In other words, a sample which was initially subjected to hydrogen activation at 250°C, followed by calcining and a second activation at 280°C, gave similar results to a sample in which the order of activation treatments was reversed. This result suggests that sulfur which migrates to the surface during hydrogen activation (see Section 3.2.) is encapsulated by a growing oxide layer during calcining, as described by Bartholomew *et al.* (*26*) in their discussion of oxygen regeneration of sulfur poisoned transition metal catalysts. Significant loss of sulfur from the catalyst during calcining, through desorption of a sulfur containing species such as SO_2, for instance, apparently does not occur, as the order in which the activation treatments are performed would affect the results if sulfur was removed by calcining.

Auger spectra were recorded using a 3-kV, 4-μA electron beam with a 100-μm spot diameter. The absence of electron beam induced sample damage over the time required to obtain a spectrum was confirmed by the fact that two spectra taken sequentially from the same sample region displayed no significant differences. Data were collected in the $E \cdot N(E)$ mode by converting the analyzer multiplier current to a proportional frequency using a Perkin–Elmer Model 96A preamplifier, and counting frequency pulses with a 24-bit counter contained in the Perkin–Elmer Model 137 PC interface. The spectra were recorded with a step size of 1 eV and a total dwell time for each step of 500 ms. Differentiation was performed using a 3-point Savitsky–Golay

convolution algorithm (*27*), which corresponds to a 2 V p/p modulation voltage in the phase sensitive detection scheme traditionally used for AES (*28*). No smoothing or other data manipulation was performed on any of the spectra. In each figure, the spectra are normalized such that the Fe(703 eV) peak heights are identical. Spectra were recorded at three different positions on each sample in order to ensure that local variations in surface composition did not give rise to unrepresentative results. In general, the samples were found to be fairly homogeneous, with Auger peak ratios varying by 20% or less across the surface. In addition, each activation was performed on three different samples. Although quantitative variations were found between different samples, the qualitative trends were reproducible.

Hydrogen (Alphagaz, research grade) and oxygen (Alphagaz, research grade) were used as received. No impurities were detected in these gases by either gas chromatography or mass spectrometry. The gas manifold was evacuated to $<10^{-5}$ Torr with a turbo pump, and flushed thoroughly with the reactant gas prior to filling of the reactor.

Nitrogen BET measurements of the surface area of the hydrogen activated catalysts were made using a Quantachrome Autosorb-6. The samples used for BET measurements were heated in air (calcined) at 300°C for 5 h in a muffle furnace, and then placed in a pyrex U-tube with a glass frit to support the sample. The U-tube was heated by a temperature-controlled furnace. The samples were activated in flowing hydrogen at 30 sccm, cooled to room temperature in vacuum, and then passivated by exposure to 2.0 Torr of air overnight prior to removal from the reduction cell and transfer to the BET bulb. In this manner, alteration of the surface area of the activated catalysts due to rapid exothermic reaction with ambient oxygen was avoided. The results of the BET measurements are shown in Table 2.

TABLE 2

BET Surface Areas of F–T Catalysts

Catalyst	Treatment	Surface area (m^2/g)
100 Fe/5 Cu/4.2 K/25 SiO_2	None	318[a]
100 Fe/5 Cu/4.2 K/25 SiO_2	H_2, 220°C, 3 h	168[a]
100 Fe/5 Cu/4.2 K/25 SiO_2	H_2, 280°C, 4 h	169
100 Fe/3 Cu/0.2 K	O_2, 300°C, 5 h	139
100 Fe/3 Cu/0.2 K	H_2, 250°C, 24 h	5–10

[a] From Ref. (*22*).

3. RESULTS AND DISCUSSION

3.1. 100 Fe/5 Cu/4.2 K/25 SiO_2 Catalyst

AES spectra of the 100 Fe/5 Cu/4.2 K/25 SiO_2 catalyst following activation in hydrogen at 220 and 280°C for 1 h are shown in Fig. 2. Peaks due to iron, copper, oxygen, silicon, and potassium are present, as expected. The copper signal is quite weak due to both the low copper content of the catalyst, as well as the low sensitivity of AES to copper (*29*). Using tabulated Auger sensitivity factors (*29*), it is found that the Cu(920 eV)/Fe(703 eV) peak ratio is close to the expected value for a homogeneous mixture of copper and iron. The potassium signal, on the other hand, is very strong even though the potassium content is similar to the copper content. This strong signal

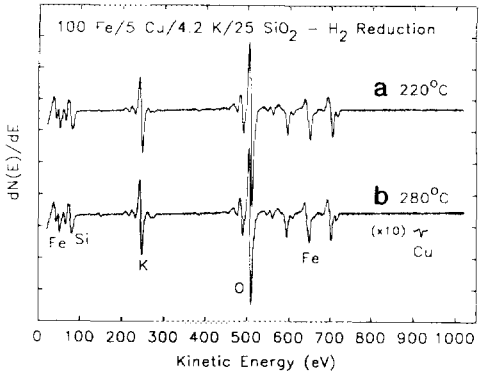

FIG. 2. Auger spectrum of the 100 Fe/5 Cu/4.2 K/25 SiO_2 catalyst following activation in one atmosphere of hydrogen for 1 h at (a) 220°C and (b) 280°C. Spectra are normalized to the Fe(703 eV) peak. The expanded Cu(920 eV) peak in (b) has been smoothed using a 5-point Savitsky–Golay smoothing algorithm (*27*).

is partly due to the high sensitivity of AES to potassium (*29*), but also to the fact that potassium is added by incipient wetness using $KHCO_3$, and therefore resides primarily on the catalyst surface. Silica is loaded by impregnation and should also reside on the catalyst surface. Since AES is very insensitive to oxidized silicon (*29*), however, the silicon Auger peak is much smaller than that of potassium even though the silicon content is substantially higher than the potassium content. The position of the silicon peak at 82 eV is higher than the known value of 76 eV for SiO_2, but substantially less than the 92 eV observed for elemental silicon (*29*), indicating that the silicon is not present as a pure SiO_2 phase. The symmetric silicon peak shape is, however, very similar to that of SiO_2 and quite different from that of elemental silicon (*29*). An iron or potassium silicate phase may explain the anomolous energy of the silicon Auger transition.

The most important conclusion to be drawn from Fig. 2 is that the spectra following the two hydrogen activation procedures are essentially indistiguishable. This observation is consistent with F–T activity measurements, which show that initial CO conversion is similar for the two hydrogen activation temperatures (*10*). Hydrocarbon selectivities do vary slightly between the two activation procedures. The catalyst activated at 280°C gave a slightly higher C_1–C_{11} yield and less C_{12}+ hydrocarbons than the catalyst activated at 220°C. The origin of these differences in catalyst selectivity cannot be ascribed to differences in catalyst morphology, as BET measurements show that the surface areas, pore volumes, and average pore sizes of the catalyst are nearly identical for the two activation temperatures. It is therefore apparent that the selectivity variation is either due to experimental uncertainty in the catalyst testing procedure, or to very subtle differences in catalyst surface composition or morphology which cannot be detected by AES or BET methods.

The iron on the catalyst surface remains in an oxidized state following hydrogen activation, as shown by the presence of a large O(511 eV) peak and the fact that the Fe(MVV) Auger region displays two peaks at 43 and 52 eV, characteristic of oxidized iron (*30–33*). Metallic iron displays only a single peak in the MVV region at 47 eV (*29–33*). Although the presence of a small amount of metallic iron cannot be ruled out, the absence of a clearly resolved peak at 47 eV indicates that the vast majority of the surface iron is oxidized. It is possible that only a thin surface oxide layer is present on the Fe/5 Cu/4.2 K/25 SiO_2 catalyst following activation, with an underlying metallic phase. This situation could occur if water generated by reduction of iron oxide were to reoxidize the catalyst surface during activation. Since the inelastic mean free path (IMFP) of the 47 eV Fe(MVV) electrons in Fe_3O_4 is only ~0.7 nm (*34*), an oxide layer would only have to be 1.5 to 2.0 nm thick to effect total attenuation of the metallic iron Auger electrons. As shown below, however, hydrogen activation of the 100 Fe/5 Cu/4.2 K/25 SiO_2 catalyst following partial removal of potassium and silica results in complete reduction of iron to the metallic state, clearly demonstrating that it is possible to obtain a completely reduced iron surface on this catalyst and to maintain this reduced state during evacuation of the reactor. It can therefore be concluded that the spectra in Fig. 2 accurately reflect the 100 Fe/5 Cu/4.2 K/25 SiO_2 catalyst surface composition following hydrogen activation. Extended hydrogen activation times up to 8 h result in no additional reduction of iron, indicating that the absence of metallic iron is not due to kinetic limitations imposed by the short, 1-h activation time.

By comparing O(511 eV)/Fe(703 eV) peak ratios of the activated catalysts with that of the calcined catalyst prior to activation (not shown) it is found that partial reduction of iron does occur during activation; the O(511 eV)/Fe(703 eV) Auger ratio drops from ~5.0 for the freshly calcined

catalyst to ~3.8 for the activated catalysts. Also, the calcined catalyst is electrically insulating, as evidenced by large shifts in the positions of the Auger peaks, requiring low electron beam currents to obtain useful Auger spectra. Following hydrogen activation, the catalyst displays good electrical conductivity such that no shifts in the Auger peaks are observed, supporting the conclusion that partial reduction occurs during hydrogen activation. Lox *et al.* (*22*) report that the 100 Fe/5 Cu/4.2 K/25 SiO_2 catalyst consists primarily of Fe_2O_3 prior to activation. It can therefore be concluded that reduction of Fe_2O_3 to Fe_3O_4 or Fe_xO occurs during hydrogen activation at 220 or 280°C. Conversion to Fe_3O_4 would be consistent with the increased electrical conductivity noted above, since the conductivity of Fe_3O_4 is 10^6 times greater than that of Fe_2O_3 (*35*). It should also be noted that the binary equilibrium phase diagram of the Fe–O system indicates that Fe_xO is not a stable phase below 570°C (*36*). It is therefore tempting to eliminate Fe_xO as a possible iron phase in the hydrogen activated 100 Fe/5 Cu/4.2 K/25 SiO_2 catalyst. Given that the catalyst is almost certainly not in an equilibrium state following hydrogen activation, and that the effects of copper and potassium on the stability of the various iron oxides is not known, this conclusion may not be warranted.

Reliable Auger reference spectra for the Fe(MVV) lineshapes of Fe_3O_4 or Fe_xO, which would allow discrimination between the two oxides, do not appear to be available in the literature. Seo *et al.* (*33*), attempted to measure Auger spectra of the various iron oxides, but, as pointed out by Brundle *et al.* (*37*), the ion bombardment used by Seo *et al.* probably caused reduction of iron to the metallic state and therefore gave misleading results. The method of Rao *et al.* (*38*), which uses ratios of the three Fe(LMM) peaks to determine oxidation states, was also inconclusive, as the ratios measured here did not correspond well with those reported by Rao *et al.* for the various iron oxides. This lack of correspondence may be the result of differences in analyzer sensitivity and transmission between the two studies. A basis for speculation as to the identity of the partially reduced iron phase is provided by the decrease in the O(511 eV)/Fe(703 eV) ratio during activation. Recall that the O(511 eV)/Fe(703 eV) ratio of the calcined catalyst is 5.0, dropping to 3.8 after activation. Since oxidation of a pure iron foil at 300°C in 130 Torr O_2 gives an O(511 eV)/Fe(703 eV) ratio of only 4.5 (*39*), that portion of the O(511 eV)/Fe(703 eV) ratio of the calcined catalyst above 4.5 must be associated with potassium and silica. Thus, assuming that no reduction of potassium or silica species occurs during activation, subtracting 0.5 from the O(511 eV)/Fe(703 eV) ratio of the activated catalyst removes the contributions due to silica and potassium species, leaving an O(511 eV)/Fe(703 eV) ratio for the iron phase only. Using this procedure shows that the O(511 eV)/Fe(703 eV) ratio of the iron phase decreases from 4.5 to 3.3 during activation. The magnitude of this decrease is less than expected for conversion of Fe_2O_3 to Fe_xO, but greater than expected for conversion to Fe_3O_4, suggesting that the surface iron phase following activation is a mixture of Fe_xO and Fe_3O_4.

Based on temperature programmed reduction (TPR), X-ray diffraction, and Mössbauer spectroscopy, Lox *et al.* (*22*) conclude that surface iron is present primarily in the Fe^{2+} oxidation state after reduction of the 100 Fe/5 Cu/4.2 K/25 SiO_2 catalyst in hydrogen at 220°C, in agreement with the present work. Interestingly, they also observe metallic iron after hydrogen reduction, but suggest that it is located in the bulk and not on the surface. As mentioned earlier, the short IMFP of the Fe(MVV) Auger electrons would prevent detection of any metallic iron located below the first few atomic layers. Li (*21*) observed substantial amounts of metallic iron in a catalyst with similar composition to the one used here, following activation in hydrogen

at 300°C for 12 h. The higher temperature and longer activation time could easily account for the greater extent of reduction observed by Li compared to the present study. Also, the use of X-ray photoelectron spectroscopy (XPS) by Li resulted in less surface sensitivity for iron than in the present study. With the Al $K\alpha$ X-ray source used in that study, the Fe $2p_{3/2}$ photoelectrons used to determine oxidation state would have kinetic energies of 770–780 eV. The IMFP of these photoelectrons in Fe_3O_4 is ~2 nm, vs only 0.7 nm for Fe(MVV) Auger electrons (*34*). As a result, if metallic iron is present in the bulk activated catalyst, as suggested by Lox *et al.* (*22*), then it would have been more likely to be detected by Li (*21*) using XPS, than in this work using AES.

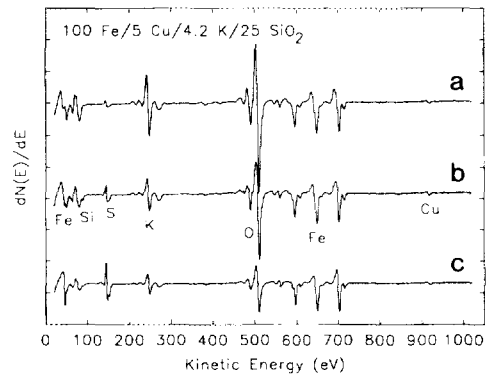

FIG. 3. Effect of lowering silica and potassium levels on the Auger spectrum of the 100 Fe/5 Cu/4.2 K/25 SiO_2 catalyst following activation in one atmosphere of hydrogen for 4 h at 250°C. Spectra are normalized to the Fe(703 eV) peak.

During the course of this investigation it was found that prolonged exposure to the electron beam results in changes in the surface composition of the 100 Fe/5 Cu/4.2 K/25 SiO_2 catalyst. In particular, removal of potassium and silicon occurs. This effect was used to investigate the effects of decreasing potassium and silica concentrations on catalyst activation. Accordingly, three different regions of a 100 Fe/5 Cu/4.2 K/25 SiO_2 catalyst sample were exposed to the electron beam (3 kV, 0.04 A/cm^2) for 0, 2, and 4 h. The sample was then calcined at 300°C for 2 h to reoxidize the silicon and iron, which were partially reduced by the electron beam exposure, and then activated at 250°C in 1 atm of hydrogen for 4 h. Results are shown in Fig. 3. As the potassium and silica coverages decrease, the extent of reduction of surface iron clearly increases, as evidenced by decreases in the O(511 eV)/Fe(703 eV) ratio as well as changes in the Fe(MVV) peak shape. Some reduction of silica may also occur on the potassium- and silica-depleted surfaces, as evidenced by the small peaks at 92 eV in curves (b) and (c). The Fe(MVV) peak shape in curve (c) of Fig. 3 indicates nearly complete reduction of surface iron to the metallic state (*30–33*), even though substantial amounts of oxygen can still be observed. This residual oxygen is associated with silica and potassium, as well as a small amount of surface iron oxide. These results clearly show that one or both of the catalyst promoters removed by electron beam exposure is responsible for inhibiting reduction of the 100 Fe/5 Cu/4.2 K/25 SiO_2 catalyst. Based on the work presented here, it is not possible to separate the effects of potassium and silica. There is evidence in the literature that both potassium (*21*, *40*) and silica (*3*, *21*, *40*, *41*) can inhibit reduction of iron catalysts. Some sulfur buildup can be seen in the reduced regions of the catalyst in Figs. 3b and 3c. The presence of this sulfur is discussed below (Section 3.2.).

3.2. 100 Fe/3 Cu/0.2 K Catalyst

Figures 4 and 5 show the effects of hydrogen activation at 250 and 280°C, respectively, on the surface composition of the 100 Fe/3 Cu/0.2 K catalyst. The spectra in Figs. 4 and 5 show Auger peaks for iron, copper, potassium, and oxygen, as expected. Minor contamination of the sample with titania and silica, combined with the weak iron Auger transition at 86 eV (*29*), give rise to the small peaks at 383, 420, and 82 eV. The contamination occured because

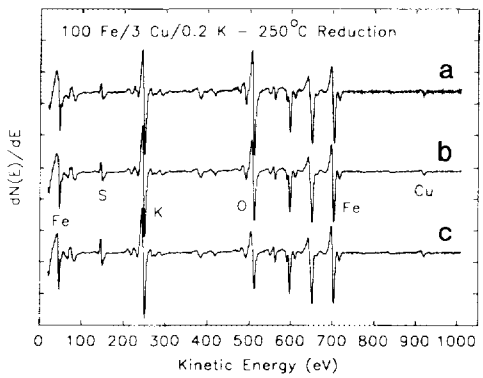

FIG. 4. Auger spectra of the 100 Fe/3 Cu/0.2 K catalyst following activation in one atmosphere of hydrogen at 250°C for (a) 4 h, (b) 10 h and (c) 22 h. Spectra are normalized to the Fe (703 eV) peak.

a die previously used with titania and silica materials was used to press the catalyst sample onto the tungsten mesh. Subsequent experiments using an uncontaminated die gave similar results, showing that the titania and silica had no effect on the catalyst behavior.

In contrast to the results for the 100 Fe/5 Cu/4.2 K/25 SiO_2 catalyst, nearly complete reduction of surface iron to the metallic state is observed for all activation times and temperatures investigated. At both temperatures, minor changes in the Fe(MVV) lineshape at 47 eV, and decreases in the O(511 eV)/Fe(703 eV) ratio for activation times greater than 4 h, indicate that a small amount of oxidized iron remains on the surface even for activation times exceeding 10 h. Li reports XPS results indicating that only 55% of the surface iron in a similar catalyst is metallic following hydrogen activation for 12 h at 300°C (*21*). In that study, however, the sample was not activated in a reactor coupled to the UHV chamber. Instead, the sample was transferred from the reactor to the sample inlet port of the UHV chamber in a glove box, with oxygen levels reported only to be less than 5 ppm. Kinetic gas theory predicts that even with an oxygen level of 1 ppm, and a very conservative estimate of 10^{-2} for the reactive sticking probability of O_2 on iron (*42*), significant buildup of oxygen would occur within a few seconds. It is therefore clear that some reoxidation of the activated sample during transfer to the XPS chamber is likely to have occurred in Li's work. This reoxidation would explain the lower level of iron reduction observed by Li than in the present study.

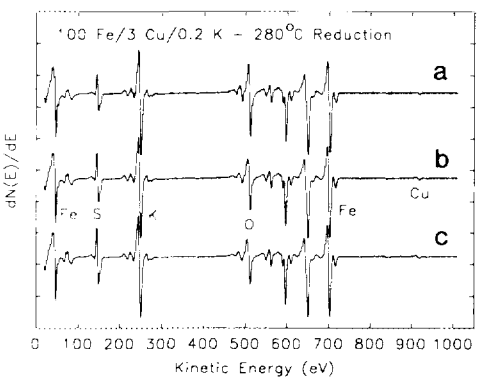

FIG. 5. Auger spectra of the 100 Fe/3 Cu/0.2 K catalyst following activation in 1 atm of hydrogen at 280°C for (a) 4 h (b) 10 h and (c) 16 h. Spectra are normalized to the Fe(703 eV) peak.

Other than slight variations in the extent of iron reduction, the only significant difference among the spectra in Figs. 4 and 5 is the sulfur coverage. Sulfur coverage is seen to increase with both activation temperature and time. For illustrative purposes, data from the sample which gave the largest sulfur signals were used to prepare Figs. 4 and 5. In two other tests with different catalyst samples, the sulfur signals were 20–30% lower than shown in the figures. The differences in extent of sulfur segregation may be due to small errors in the temperature measurements, resulting from the fact that the thermocouple was not in direct contact with the catalyst samples. The source of the sulfur is most likely a bulk impurity in the catalyst, which segregates to the surface upon reduction of the iron. The metal nitrates used to prepare the precipitated iron catalysts contain small amounts of sulfate as an impurity (*43*). Li

(*21*) does not report the presence of sulfur on a 100 Fe/3 Cu/0.2 K catalyst following activation, but it is not clear whether the S 2*p* region was investigated. Wachs *et al.* (*4*), did observe ~0.03 monolayers (ML) of sulfur on a hydrogen activated 100 Fe/1.6 Cu catalyst prepared from Fe_2O_3 powder (Baker, 99.9%), but suggest that this sulfur coverage is too low to be significant.

Quantification of sulfur coverages using tabulated Auger sensitivity factors (*29*) and the methodology described by Briggs and Seah (*44*) indicates that typical S(150 eV)/Fe(703 eV) Auger peak ratios measured for the activated catalysts correspond to 0.07–0.18 ML of sulfur. Since a typical sulfate impurity level in the $Fe(NO_3)_3 \cdot 9H_2O$ used to synthesize the catalyst is 0.01 wt% (*43*), and the BET surface areas of the hydrogen activated catalysts vary from 5 to 10 m^2/g, it can be shown that the maximum sulfur coverage on this catalyst, assuming that all of the iron is completely reduced and all of the sulfur migrates to the surface, is on the order of 0.04–0.09 ML. Given the uncertainties in Auger sensitivity factors and poor reproducibility in the BET measurements, the factor of 2 difference between the maximum calculated sulfur coverage and the maximum measured coverage is not believed to be significant. Sulfur impurities in the starting materials are therefore large enough to account for the observed sulfur coverages. Nevertheless, a blank experiment was conducted in which a bare tungsten grid was mounted in the apparatus and subjected to hydrogen activation conditions. No sulfur was detected on the surface of the grid after activation, demonstrating that sulfur impurities are absent from the tungsten grid and the hydrogen gas, and that there is no contamination in the apparatus itself which could give rise to sulfur on the catalyst surface.

Comparison of the sulfur levels in Figs. 4 and 5 with the CO conversions measured for the various activation procedures (Table 1) shows that CO conversion is inversely related to sulfur coverage, consistent with the well-known poisoning effect of sulfur on the F–T reactions (*3*, *45*). Evidently sulfur does not affect F–T selectivity for this catalyst, as all four hydrogen activation conditions result in similar selectivities (*11*). Based on measurements of CO methanation on sulfur modified single crystal metal surfaces (*46*), which show that 0.1 ML of sulfur can decrease methanation rates by an order of magnitude, the measured sulfur coverages of 0.07–0.18 ML are certainly high enough to have the observed effect on the rate of the F–T reaction. Thus, the variations in sulfur coverage observed following hydrogen activation of the 100 Fe/3 Cu/0.2 K catalyst are alone capable of giving rise to the observed variations in CO conversion during F–T synthesis, and no additional factors need be considered to explain the variation of catalyst activity with activation temperature and time. It is important to note, however, that surface area differences may also contribute to the differences in activity. Activation at 280°C appears to result in somewhat lower surface areas than activation at 250°C. Unfortunately, the BET measurements on the activated 100 Fe/3 Cu/0.2 K catalysts were not very reproducible, so the magnitude of the surface area difference is not known. Thus, it must be concluded that while sulfur contamination appears to be a primary cause of the observed F–T activity differences, surface area differences may also contribute. In fact, the two effects may be inseparable, as a decrease in surface area would result in an increase in the maximum possible sulfur coverage.

Since the source of the sulfur is bulk impurities in the catalyst starting materials, it is clear that sulfur poisoning can be a problem for F–T catalysts, even in the absence of sulfur in the reactor feed. Thus, at least for this particular catalyst, hydrogen activation should be performed at the lowest temperature possible to minimize sulfur segregation to the surface, while at the same time ensuring complete or nearly complete reduction of iron to the metallic

state. The results of this study also show that rigorous exclusion of sulfur impurities from the $Fe(NO_3)_3$ used to prepare the catalyst would have a beneficial effect on catalyst performance following hydrogen activation.

It is not clear how far the results of this study can be generalized. As mentioned above, Wachs *et al.* (*4*) also observed sulfur segregation during hydrogen activation of an F–T catalyst, and, given the voluminous literature on F–T catalysis, it is certainly possible that additional instances of sulfur segregation have been reported. It is likely that the effects of sulfur segregation are often masked by other processes occuring during hydrogen activation. In addition to questions of sulfur segregation, the extent of iron reduction and changes in catalyst surface area must also be considered when comparing the effects of different activation procedures. For instance, Blanchard *et al.* (*47*), find that hydrogen activation of an unsupported Fe_2O_3 powder at 500°C gives much lower activity than activation at 250°C, in seeming agreement with the results of this paper. Surface area measurements show, however, that the differences in activity are largely due to a difference of nearly two orders of magnitude in catalyst surface area between the two activation procedures. Thus, while sulfur segregation during hydrogen activation of iron F–T catalysts can have important consequences for catalyst activity, these effects may only be observable in instances where variations in activation conditions do not strongly perturb the catalyst surface area or the extent of iron reduction.

Little has been said so far regarding changes in K(252 eV)/Fe(703 eV) ratios during activation. This lack of discussion is due to the presence of two competing effects which make interpretation of changes in this ratio difficult. First, substantial surface area is lost upon reduction, resulting in an increase in the coverage of the potassium promoter, which resides primarily on the surface of the catalyst. This effect tends to *increase* K(252 eV)/Fe(703 eV) ratios. Second, reduction of the iron to the metallic state results in shrinkage of the catalyst particles due to removal of oxygen. As a result, the density of iron atoms increases. Since the Fe(703 eV) Auger peak contains contributions from iron atoms within 2 to 3 nm of the surface, the increase in iron atom density causes a corresponding increase in the Fe(703 eV) peak height. This effect tends to *decrease* K(252 eV)/Fe(703 eV) ratios. Experimentally, it is found that K(252 eV)/Fe(703 eV) ratios decrease upon hydrogen activation, suggesting that increases in the Fe(703 eV) ratio due to an increase in the density of iron atoms dominates over increases in surface coverage of potassium due to loss of surface area. Furthermore, the possibility that the distribution of potassium species may change during activation, e.g., through island formation, also complicates interpretation of K(252 eV)/Fe(703 eV) ratios.

In spite of these difficulties, it is still possible to gain information on the stoichiometry of the potassium–oxygen surface complex. The Fe(MVV) peak shapes at 47 eV in Figs. 4 and 5 can be matched to peak shapes for partially oxidized iron foils (*39*), allowing the O(511 eV)/Fe(703 eV) ratio corresponding to the given Fe(MVV) peak shape to be found. This ratio is then subtracted from the O(511 eV)/Fe(703 eV) ratio measured for the activated catalyst, and the resulting value is divided by the K(252 eV)/Fe(703 eV) ratio to give the O(511 eV)/K(252 eV) ratio of the potassium-oxygen complex. This calculation assumes that copper is completely reduced following activation, a reasonable assumption given that the function of copper is to enhance reduction (*1–4*) and that TPR indicates that copper reduction precedes iron reduction (*4*, *21*). The results of this calculation are given in Table 3. For both activation temperatures, the ratio decreases with time, demonstrating that reduction of potassium is occurring. Not surprisingly, the extent of potassium reduction is greater at 280°C

TABLE 3

O(511 eV)/K(252 eV) Auger Peak Ratios for Potassium-Oxygen Complex in 100 Fe/3 Cu/0.2 K Catalyst

Activation	$(O/Fe)_{Fe}$[a]	$(O/Fe)_{cat}$[b]	$(O/Fe)_K$[c]	$(K/Fe)_{cat}$[d]	$(O/K)_K$[e]
H_2, 250°C, 4 h	0.57	1.37	0.80	1.37	0.58
H_2, 250°C, 10 h	0.40	1.03	0.63	1.43	0.44
H_2, 250°C, 22 h	0.27	0.75	0.48	1.42	0.34
H_2, 280°C, 4 h	0.44	0.80	0.36	1.16	0.31
H_2, 280°C, 10 h	0.37	0.57	0.20	1.11	0.18
H_2, 280°C, 16 h	0.31	0.50	0.19	1.11	0.17

[a] O(511 eV)/Fe(703 eV) peak ratio due to iron oxide (see text for details).

[b] O(511 eV)/Fe(703 eV) peak ratio of the activated catalyst.

[c] O(511 eV)/Fe(703 eV) peak ratio due to oxygen in the potassium complex. $((O/Fe)_{cat}-(O/Fe)_{Fe})$

[d] K(252 eV)/Fe(703 eV) peak ratio of the activated catalyst.

[e] O(511 eV)/K(252 eV) peak ratio of the potassium–oxygen complex in the activated catalyst. $((O/Fe)_K/(O/Fe)_{cat})$

than at 250°C. Regretably, the oxygen Auger peak shape varies greatly with chemical environment (*29*), and as a result, tabulated oxygen Auger sensitivity factors are not very useful. This difficulty prevents a quantitative determination of the O/K atomic ratio of the potassium species. Knowing that the maximum possible ratio of oxygen to potassium is 1 : 1 (for KOH), however, the decrease in the Auger ratio shown in Table 3 clearly shows that a majority of the potassium is reduced to the elemental state after hydrogen activation at 280°C for 24 h. The K(252 eV) peak shape does not change noticeably as a result of reduction since elemental potassium adsorbed on transistion metal surfaces donates substantial charge to the surface, and therefore has an electronic structure very similar to that of ionic potassium (*48*). Under actual Fischer–Tropsch reaction conditions the potassium would undoubtedly be reoxidized to KOH by water generated by the reaction and by oxygen atoms generated by CO dissociation (*5*, *7*, *17*).

3.3. Comparison of 100 Fe/5 Cu/4.2 K/25 SiO_2 and 100 Fe/3 Cu/0.2 K Catalysts

It is useful to compare the behavior of the two catalysts used in this study to determine why the 100 Fe/5 Cu/4.2 K/25 SiO_2 catalyst displays little variation in F–T activity with hydrogen activation temperature, while the 100 Fe/3 Cu/0.2 K catalyst displays a very strong dependence of activity on activation temperature. The most obvious difference between the two catalysts lies in the reduction behavior. While the 100 Fe/3 Cu/0.2 K catalyst undergoes complete reduction during hydrogen activation, the 100 Fe/5 Cu/4.2 K/25 SiO_2 catalyst is only partially reduced. The lack of reduction for the 100 Fe/5 Cu/4.2 K/25 SiO_2 catalyst has two possible consequences which could help explain the invariance of activity with hydrogen activation temperature. First, it is possible that the sulfur impurities are unable to segregate to the surface of the oxide phase. This situation could occur if the sulfur is immobile in the oxide phase, or if the surface free energy of the sulfur impurity is less than that of the oxide phase, so that no thermodynamic driving force exists for segregation of sulfur to the surface. Second, in the absence of reduction, the surface area of the activated 100 Fe/5 Cu/4.2 K/25 SiO_2 catalyst remains quite high at 170 m^2/g, 17–34 times greater than that of the activated 100 Fe/3 Cu/0.2 K catalysts. As a result, even if all of the sulfur impurities were to segregate to the surface of the 100 Fe/5 Cu/4.2 K/25 SiO_2 catalyst, the sulfur coverage would still be less than 0.01 ML, hardly enough to have a major effect on catalyst activity. Indeed, Fig. 2b shows a very small sulfur peak which is about the right magnitude to be due to segregated sulfur. In either case, the absence of significant sulfur poisoning of the 100 Fe/5 Cu/4.2 K/25 SiO_2 catalyst, together with the fact that 280°C is not high enough to overcome the barrier to reduction of the oxide phase, results in the absence of any major differences between activation in hydrogen at 220 and 280°C. The substantial sulfur coverages seen in Fig. 3 for the potassium and silica depleted 100 Fe/5 Cu/4.2 K/25 SiO_2 catalyst suggest that the surface area of this catalyst decreases dramatically upon

reduction of iron to the metallic state, similar to the loss of surface area seen for the 100 Fe/3 Cu/0.2 K catalyst upon hydrogen activation. Unfortunately, it is not possible to remove potassium and silica from the bulk 100 Fe/5 Cu/4.2 K/25 SiO_2 catalyst, so a BET experiment cannot be performed to confirm the surface area loss.

In contrast to the 100 Fe/5 Cu/4.2 K/25 SiO_2 catalyst, the 100 Fe/3 Cu/0.2 K catalyst is extensively reduced at both 250 and 280°C, resulting in a substantial loss of surface area. As a result, sulfur segregation results in sulfur coverages on the surface which are large enough to alter catalyst activity. Because the rate of sulfur segregation depends on temperature, the sulfur coverage varies as a function of temperature, resulting in substantial variations in F–T activity with hydrogen activation temperature.

Based on the above discussion it can be seen that any changes in the activation procedure which serve to maintain catalyst surface areas would have a beneficial effect on catalyst performance not only by increasing active surface area, but also by lowering the maximum sulfur coverage which could result from sulfur segregation. Indeed, addition of silica to F–T catalysts is primarily intended to stabilize surface area, although the experiments reported here and elsewhere show that silica may have chemical as well as structural effects on catalyst properties (*3*, *21*, *40*, *41*).

It is perhaps surprising that the 100 Fe/5 Cu/4.2 K/25 SiO_2 catalyst and the 100 Fe/3 Cu/0.2 K catalyst both display similar F–T activities when tested under similar conditions (see Table 1). Since the surface compositions of the two catalysts are so radically different, the F–T activities might also be expected to be quite different. In fact, the activities are very different if the comparison is made on the basis of activity per unit area of catalyst, since the surface area of the activated 100 Fe/5 Cu/4.2 K/25 SiO_2 catalyst is much higher than that of the activated 100 Fe/3 Cu/0.2 K catalyst. It therefore appears that the partially reduced iron phase formed by activation of the 100 Fe/5 Cu/4.2 K/25 SiO_2 catalyst is much less active than the metallic or carbidic iron phase formed by activation of the 100 Fe/3 Cu/0.2 K catalyst. It is even possible that the partially reduced iron phase present in the 100 Fe/5 Cu/4.2 K/25 SiO_2 catalyst is completely inactive, and the F–T activity of this catalyst is due to a small amount of metallic iron which is undetectable by AES.

4. CONCLUSIONS

The effects of hydrogen activation on the surface composition of two different iron F–T catalysts have been studied. For both catalysts, the surface composition correlates well with activity measurements performed on the same catalysts. For a 100 Fe/5 Cu/4.2 K/25 SiO_2 catalyst, no significant variation in surface composition is seen as a function of hydrogen activation temperature, in agreement with the fact that measured initial CO conversion over this catalyst is also independent of activation temperature. For both activation temperatures studied with this catalyst, only partial reduction of the surface iron to a mixture of Fe_xO and Fe_3O_4 is observed, and no evidence for metallic iron is seen. Using electron beam effects to lower silica and potassium levels increases the ease of reduction of iron, demonstrating that one or both of these components is responsible for inhibiting iron reduction in the 100 Fe/5 Cu/4.2 K/25 SiO_2 catalyst.

In contrast to the 100 Fe/5 Cu/4.2 K/25 SiO_2 catalyst, a 100 Fe/3 Cu/0.2 K catalyst displays significant variations in activity with activation procedures, and these differences are reflected in the surface composition. For hydrogen activation, essentially complete reduction to the metallic state is observed for all activation times and temperatures. In addition, migration of bulk sulfur impurities to the surface occurs during activation. The surface sulfur concentrations correlate inversely with catalyst activity, consistent with the known poison-

ing effect of sulfur on F–T activity. This result demonstrates that sulfur poisoning can be a problem for iron F–T catalysts even in the absence of sulfur impurities in the reactor feed. Rigorous exclusion of sulfur impurities from starting materials used in catalyst preparation would therefore have a beneficial effect on catalyst performance. Also, the present study suggests that hydrogen activation should be performed at the lowest temperature possible to minimize sulfur segregation, while at the same time ensuring complete or nearly complete reduction of surface iron to the metallic state.

The differences between the two catalysts are related to their reduction behavior during activation. The 100 Fe/5 Cu/4.2 K/25 SiO_2 catalyst does not reduce completely during activation, and, as a result, maintains a high surface area. The 100 Fe/3 Cu/0.2 K catalyst, on the other hand, undergoes essentially complete reduction, resulting in a dramatic loss of surface area. The large difference in surface area between the two activated catalysts means that while segregation of bulk impurities results in significant sulfur coverages for the 100 Fe/3 Cu/0.2 K catalyst, sulfur coverage is negligible for the 100 Fe/5 Cu/4.2 K/25 SiO_2 catalyst. As a result, the 100 Fe/5 Cu/4.2 K/25 SiO_2 catalyst is insensitive to activation conditions, while the 100 Fe/3 Cu/0.2 K catalyst displays wide variations in F–T activity with activation conditions. Differences in the rate of sulfur segregation with temperature result in differences in sulfur coverage for the 100 Fe/3 Cu/0.2 K catalyst, and these differences in sulfur coverage give rise to the observed variations in F–T activity with activation conditions for this catalyst.

In the following paper (9), the effects of carbon monoxide activation on the surface composition of these two F–T catalysts will be reported. It is shown there that although the effects of CO activation are generally more complicated than hydrogen activation, it is still possible to correlate changes in surface composition with changes in F–T activity.

ACKNOWLEDGMENTS

The author thanks Professor Dragomir Bukur of Texas A&M University for providing the catalyst sample used in this work, as well as for many stimulating discussions. The technical assistance of Elaine Boespflug is also gratefully acknowledged. Support for this work was provided by the Fossil Energy Division of the U.S. Department of Energy.

REFERENCES

1. Rao, V. U. S., Steigel, G. J., Cinquegrane, G. J., and Srivastava, R. D., *Fuel Process. Technol.* **30,** 83 (1992).
2. Bukur, D. B., Mukesh, D., and Snehal, A. P., *Ind. Eng. Chem. Res.* **29,** 194 (1990).
3. Dry, M. E., *in* "Applied Industrial Catalysis" (Bruce E. Leach, Ed.), Vol. 2, p. 167. Academic Press, New York, 1983.
4. Wachs, I. E., Dwyer, D. J., and Iglesia, E., *Appl. Catal.* **12,** 201 (1984).
5. Dwyer, D. J., and Hardenburgh, J. H., *Appl. Surf. Sci.* **19,** 14 (1984).
6. Bonzel, H. P., and Krebs, H. J., *Surf. Sci.* **109,** L527 (1981).
7. Wesner, D. A., Coenen, F. P., and Bonzel, H. P., *Langmuir* **1,** 478 (1985).
8. Frohning, C. D., *in* "New Syntheses with Carbon Monoxide" (J. Falbe, Ed.), p. 353. Springer-Verlag, New York, 1980.
9. Sault, A. G., and Datye, A. K., *J. Catal.* **140,** 136–149 (1993).
10. Bukur, D. B., Ledakowicz, S., and Rama Krishna, M., *in* "Indirect Liquefaction Contractors' Review Meeting Proceedings" (G. J. Steigel and R. D. Srivastava, Eds.), p. 221. U.S. Department of Energy, Pittsburgh Energy Technology Center, Pittsburgh, 1990. (Available from the National Technical Information Service, U.S. Dept. of Commerce, Springfield, VA 22161.)
11. Bukur, D. B., Lang, X., Rossin, J. A., Zimmerman, W. H., Rosnyek, M. P., Yeh, E. B., and Li, C., *Ind. Eng. Chem. Res.* **28,** 1130 (1989).
12. Dwyer, D. J., and Hardenburgh, J. H., *J. Catal.* **87,** 66 (1984).
13. Dwyer, D. J., and Somorjai, G. A., *J. Catal.* **52,** 291 (1978).
14. Dwyer, D. J., and Hardenburgh, J. H., *Prepr. Am. Chem. Soc. Div. Fuel Chem.* **31**(2), 215 (1986).
15. Bonzel, H. P., and Krebs, H. J., *Surf. Sci.* **99,** 570 (1980).
16. Bonzel, H. P., and Krebs, H. J., *Surf. Sci.* **91,** 499 (1980).
17. Bonzel, H. P., Borden, G., and Krebs, H. J., *Appl. Surf. Sci.* **16,** 373 (1983).

18. Bonzel, H. P., Krebs, H. J., and Schwarting, W., *Chem. Phys. Lett.* **72,** 165 (1980).
19. Krebs, H. J., Bonzel, H. P., Schwarting, W., and Gafner, G., *J. Catal.* **72,** 199. (1981).
20. Kuivila, C. S., Stair, P. C., and Butt, J. B., *J. Catal.* **118,** 299 (1989).
21. Li, C., "Effect of Potassium and Copper Promoters on Reduction Behavior of Precipitated Iron Catalysts." Ph.D. Thesis, Texas A&M University, 1988.
22. Lox, E. S., Marin, G. B., DeGrave, E., And Bussiere, P., *Appl. Catal.* **40,** 197 (1988).
23. Copperthwaite, R. G., Loggenberg, P. M., Derry, T. E., and Sellschop, J. P. F., *Vacuum* **38,** 413 (1988).
24. Loggenberg, P. M., Copperthwaite, R. G., Everson, R. C., and Sellschop, J. P. F., *Appl. Surf. Sci.* **31,** 327 (1988).
25. Bukur, D. B., Private communication.
26. Bartholomew, C. H., Agrawal, P. K., and Katzer, J. R., *Adv. Catal.* **31,** 135 (1982).
27. Savitsky, A., and Golay, M. J. E., *Anal. Chem.* **36,** 1627 (1964).
28. Seah, M. P., Anthony, M. T., and Dench, W. A., *J. Phys. E: Sci. Instrum.* **16,** 848 (1983).
29. Davis, L. E., McDonald, N. C., Palmberg, P. W., Raich, G. E., and Weber, R. E., "Handbook of Auger Electron Spectroscopy," Perkin–Elmer Corp., Eden Prairie, MN, 1978.
30. Arbab, M., and Hudson, J. B., *Surf. Sci.* **206,** 317 (1988).
31. Simmons, G. W., and Dwyer, D. J., *Surf. Sci.* **48,** 373 (1975).
32. Miyano, T., Sakisaka, Y., Komeda, T., and Onchi, M., *Surf. Sci.* **169,** 197 (1986).
33. Seo, M., Lumsden, J. B., and Staehle, R. W., *Surf. Sci.* **50,** 541 (1975).
34. Seah, M. P., and Dench, W. A., *Surf. Interface Anal.* **1,** 2 (1979).
35. Cotton, F. A., and Wilkinson, G., "Advanced Inorganic Chemistry," 4th ed., p. 753. Wiley, New York, 1980.
36. Massalski, T. B., "Binary Alloy Phase Diagrams." 2nd ed. ASM International, Materials Park, OH, 1990.
37. Brundle, C. R., Chuang, T. J., and Wandelt, K., *Surf. Sci.* **68,** 459 (1977).
38. Rao, C. N. R., Sarma, D. D., and Hegde, M. S., *Proc. R. Soc. London Ser. A* **370,** 269 (1980).
39. Sault, A. G., in preparation.
40. Rankin, J. L., and Bartholomew, C. H., *J. Catal.* **100,** 533 (1986).
41. Dalmon, J.-A., Dutartre, R., and Martin, G.-A., *C. R. Acad. Sci. Ser. C* **287,** 557 (1978).
42. Leygraf, C., and Ekelund, S., *Surf. Sci.* **40,** 609 (1973).
43. American Chemical Society, "Reagent Chemicals," 7th ed., p. 293. American Chemical Society, Washington, DC, 1986.
44. Briggs, D., and Seah, M. P., "Practical Surface Analysis by Auger and X-ray Photoelectron Spectroscopy," Chap. 5. Wiley, New York, 1983.
45. Anderson, R. B., "The Fischer Tropsch Synthesis," p. 230. Academic Press, New York, 1984.
46. Sault, A. G., and Goodman, D. W., *in* "Molecule Surface Interactions" (K. P. Lawley, Ed.), p. 153. Wiley, New York, 1989.
47. Blanchard, F., Reymond, J. P., Pommier, B., and Teichner, S. J., *J. Mol. Catal.* **17,** 171 (1982).
48. Bonzel, H. P., *Surf. Sci. Rep.* **8,** 43 (1988).